Routes to Chaos in the Peroxidase–Oxidase Reaction: Period-Doubling and Period-Adding

ARTICLE *in* THE JOURNAL OF PHYSICAL CHEMISTRY B · JUNE 1997

Impact Factor: 3.3 · DOI: 10.1021/jp9707549

Routes to Chaos in the Peroxidase−Oxidase Reaction: Period-Doubling and Period-Adding

Marcus J. B. Hauser,[†] Lars F. Olsen,*[,†] Tatiana V. Bronnikova,[‡,§] and William M. Schaffer[‡]

Physical Biochemistry Group, Institute of Biochemistry, Odense University, Forskerparken 10, DK-5230 Odense M, Denmark, and Department of Ecology and Evolutionary Biology, University of Arizona, Tucson, Arizona 85721

Received: February 28, 1997; In Final Form: April 16, 1997[⊗]

Previous investigations of the peroxidase−oxidase reaction indicate the existence of a period-doubling route to chaos at pH 5.2 and a period-adding route at pH 6.3. In the present study, we extend these results in two regards: (i) The reaction was studied at a series of intermediate pH values under otherwise identical conditions. The new experiments suggest that the transition from period-doubling to period-adding takes place at approximately pH 5.4 and is characterized by a loss of dynamical complexity. (ii) A detailed model (Bronnikova, T. V.; Fed'kina, V. R.; Schaffer, W. M.; Olsen, L. F. *J. Phys. Chem.* **1995**, *99*, 9309−9312) was shown capable of reproducing the principal experimental results. These include the shift from period-doubling to period-adding, the existence of narrow regions of period-doubling between adjacent mixed-mode oscillations in the period-adding regime and changes in cycle amplitude.

I. Introduction

In recent years, the peroxidase-catalyzed oxidation of reduced nicotinamide adenine dinucleotide (NADH) by molecular oxygen has become a model system for the study of complex dynamics in a biochemical context. Peroxidases catalyze the oxidation of a large number of hydrogen donors. Typically, the oxidizing agent is H_2O_2, but for some substrates, *e.g.*, NADH, molecular oxygen can serve in its place. Such reactions are called peroxidase−oxidase (PO) reactions. With NADH as the hydrogen donor, the overall stoichiometry is

$$2\mathrm{NADH} + \mathrm{O_2} + 2\mathrm{H^+} \rightarrow 2\mathrm{NAD^+} + 2\mathrm{H_2O}$$

The PO reaction is typically studied under semibatch conditions or in continuous-flow stirred tank reactors. In the former case, NADH and O_2 are supplied to a reactor in which products accumulate; in the latter, all reactants, including the enzyme, are fed into the reaction vessel, and products are removed via the overflow of excess liquid. In both circumstances, the PO reaction displays a rich variety of dynamic behaviors,[1] including bistability,[2,3] periodic oscillations[4−7] (including mixed-mode oscillations (MMO's)[8−10]), quasiperiodicity,[8,11] and at least two distinct forms of chaotic behavior.[9,10,12,13]

Traditionally, the PO reaction is studied in the presence of the modifiers methylene blue (MB) and 2,4-dichlorophenol (DCP). In this regard, it has been suggested that DCP acts as an enzyme activator,[12] whereas MB functions as an inhibitor[4,5] that plays a role in regulating the formation of ferrous peroxidase.[14] Even though simple oscillations have now been reported[15,16] in the absence of each of these compounds, more complex behaviors require the presence of both substances. Of relevance to the reaction's possible role in the metabolism of living cells is the observation that several other aromatic compounds can substitute for DCP without compromising the system's ability to display complex dynamics.[17]

The natural context in which to view dynamical diversity in the PO reaction is the theory of nonlinear dynamics,[18−20] which, among other things, emphasizes the transitions (bifurcations) from one dynamical regime to another and, more generally, the sequences of bifurcations that may be obtained in response to smoothly varying a parameter. Of particular interest are the so-called "routes to chaos," *i.e.*, bifurcation sequences which culminate in chaotic behavior.[21] Of these, the most familiar is the "period-doubling scenario" which achieved prominence as a result of pioneering studies by May[22] and Feigenbaum.[23,24] Here, a periodic orbit undergoes successive period-doubling bifurcations in response to progressively smaller and smaller changes in a control parameter until the attainment of an accumulation point—at which value the period becomes infinite. It is important to note that the dynamics at this point, while ergodic, are *not* chaotic;[25] *i.e.*, nearby trajectories do not diverge exponentially. Often, however, the accumulation point is followed by a parameter regime in which periodic and chaotic states succeed each other in a complicated fashion. Even in frequently studied one-dimensional maps for which one can show rigorously[26] that the preponderance of parameter values in this region correspond to periodic states, computer simulations generally suggest a region of chaotic behavior interrupted by subintervals of cyclic dynamics, the so-called "periodic windows".[27] In such cases and, as a matter of convenience, the entire range of parameter values is commonly referred to as the "chaotic region", and, since this region follows an initial period-doubling cascade, one encounters the term "period-doubling to chaos".

Sometimes it is possible to say something about the ordering of the periodic states within the chaotic region. For certain one-dimensional maps, the results of Metropolis, Stein, and Stein[28] apply, in which case, the sequence of base cycles (and hence the windows) conforms to the U-sequence.[29] Generally speaking, the most prominent windows are those associated with the base cycles of lowest period—hence the interpretation of experimentally observed period-3 cycles[30] as further evidence of "period-doubling to chaos." In sum, the term "period-doubling route to chaos" implies a bifurcation scenario of the sort observed in the most commonly studied unimodal maps, *i.e.*,

* Author to whom correspondence should be sent. Fax: +45 - 65 93 23 09. email:lfo@dou.dk.
[†] Odense University.
[‡] University of Arizona.
[§] Permanent address: Institute of Theoretical and Experimental Biophysics, Russian Academy of Sciences, Pushchino 142292, Moscow Region, Russia.
[⊗] Abstract published in *Advance ACS Abstracts,* June 1, 1997.

S1089-5647(97)00754-2 CCC: $14.00

an accumulating cascade of period-doubling bifurcations followed by a region of complex dynamics punctuated by periodic windows, the ordering of which sometimes conforms to the U-sequence.

A second well-known route to chaos is the "torus route" which involves periodic or quasiperiodic motion on invariant tori.[31,32] In this case, there are typically two parameters, and the control plane is divided into locking regions, the so-called "Arnol'd tongues",[33,34] delimited by saddle-node bifurcations. Within these regions, one often observes period-doubling to chaos as described above. By judiciously varying a parameter, one may thus obtain complicated sequences of periodic and aperiodic states. Here, the analogue of the U-sequence is the Farey sequence, whereby the ordering of the locking regions corresponds to elements of a Farey series. By this, we mean that the sequence of their rotation numbers, $\rho = p/q$, satisfies the operation of Farey addition, *i.e.*,

$$p_1/q_1 \oplus p_2/q_2 = p_3/q_3 = (p_1 + p_2)/(q_1 + q_2)$$

The implication is that if there exists a parameter value, μ_3, corresponding to a cycle, Γ_3, for which $\rho_3 = p_3/q_3$, it will be sandwiched between two other values, μ_1 and μ_2, corresponding to cycles, Γ_1 and Γ_2, for which $\rho_1 = p_1/q_1$ and $\rho_2 = p_2/q_2$. This property gives rise to the notion of the "Farey tree", the levels of which correspond to $p = 1, 2, 3, ...$[35] Interestingly, the number of levels can depend on a parameter; in which regard, Ringland *et al.*[36] showed that it is possible to go from bifurcation sequences involving only the top level of the tree, *i.e.*, cycles with rotation numbers 1/1, 1/2, 1/3, ..., to sequences involving multiple levels. Note that a sequence involving only the top level amounts to *period-adding*.

Experimentally, period-doubling and period-adding sequences have been reported in the PO reaction. The former predominates at pH values around 5,[13,37] while the latter is observable at pH values around 6.[10] We stress that the two scenarios are observable under identical conditions save for the difference in pH.[37] In the present paper, we study the reaction's behavior at intermediate pH values with an eye toward documenting how one bifurcation sequence gives way to the other. We also show that the principal experimental results can be reproduced by a detailed model[38] of the reaction.

The remainder of the paper is organized as follows: Section II gives materials and methods. In section III, we present the experimental results. Here we show that the transition from period-doubling to period-adding occurs at a pH of approximately 5.4 and is marked by an associated loss of dynamical complexity. In section IV, we attempt to reproduce these results on the computer using a recently proposed detailed model[38] of the reaction. The calculations turn out to be in broad qualitative agreement with the experimental findings. The model further predicts that the narrow regions of complex dynamics observed at high pH between adjacent MMO's result from homoclinic transitions to chaos of a novel type. A detailed analysis of these transitions will be presented in a following article.[39]

II. Experimental Section

Experiments were performed in a quartz cuvette (21.7 × 21.7 × 42 mm) equipped with an oxygen electrode. The cuvette was placed in a Zeiss Specord S10 diode array spectrophotometer. Only the photometer's tungsten lamp was used as light source in order to avoid photochemical reactions induced by UV irradiation.[7,40] Oxygen concentration, as well as the absorbencies of NADH (at 360 nm), native ferric peroxidase (403 nm), oxyferrous peroxidase (compound III; 418 nm), and ferrous peroxidase (439 nm) were recorded every 2 s and stored in a computer for later analysis.

The reactor had a liquid volume of 10 mL as well as an approximately 10 mL gas phase above the reaction mixture. The reaction mixture contained 0.1 μM methylene blue, 25.0 μM 2,4-dichlorophenol, and 1.3−1.6 μM horseradish peroxidase, in 0.1 M buffer (0.1 M acetate buffer for experiments at pH 5.2−5.9; 0.1 M phosphate buffer for experiments at pH 6.1−6.3). A 0.1 M aqueous solution of NADH was delivered to the reaction vessel at constant flow rates through a capillary tube connected to a syringe pump. The volume of the added solution during each experiment was negligible and balanced by an equal volume of water evaporated. Thus, the liquid volume was effectively constant at 10 mL throughout the experiment. Oxygen was supplied at atmospheric pressure to the reaction mixture via a gas mixer. The moisturized O_2/N_2 stream contained 1.05% (v/v) oxygen. The rate of oxygen diffusion ν into the liquid is given by

$$\nu = K([O_2]_{eq} - [O_2])$$

where $[O_2]$ is the oxygen concentration in solution; $[O_2]_{eq}$, the oxygen concentration at equilibrium, and K, the oxygen transfer constant. For a stirring rate of 1050 rpm K was determined to be $6.0 \times 10^{-3} \pm 0.2 \times 10^{-3}$ s^{-1}.

Prior to the start of each experiment, the reaction mixture containing enzyme, MB, and DCP in buffer was thermostated at 28.0 ± 0.1 °C and equilibrated with pure nitrogen. Experiments were typically started by adding NADH at a flow rate of 60 μL h^{-1}. As the absorbance at 360 nm reached a level close to the NADH concentration associated with a given dynamic state, the composition of the gas stream was switched from pure N_2 to the O_2/N_2 mixture. Then the NADH flow-rate was adjusted (50−70 μL h^{-1}) such that the NADH concentration oscillated around a constant mean level corresponding to this particular dynamic state. The dynamics were then recorded over a period of time. Thereafter, the pumping rate was changed to allow the NADH concentration to settle to another mean level associated with a different behavior. Thus, changing the mean NADH concentration allows for the observation of different dynamical states as well as an unambiguous determination of the order in which they occur. Accordingly, we use the mean NADH concentration as a bifurcation parameter. One could also use the NADH flow rate, which, of course, determines the average NADH concentration, although the relation between the two is nonlinear. But this approach, while it makes for a somewhat more straightforward comparison of the data and the simulations, is less reliable. This is because, in spite of great precautions to prepare identical NADH stock solutions, small variations in NADH stock solutions are unavoidable. If uncontrolled, these variations will necessarily affect the dynamics and are consequently a potential source of error. In short, the use of mean NADH concentration as described here removes an otherwise inevitable source of inter-experiment variability.

The pK_a values of nicotinamide adenine dinucleotide (NAD^+) and its reduced form, NADH, were determined by pH titration. Solutions of 2.6 μmol NADH disodium salt in 3.0 mL of 0.05 M NaCl were titrated against either 0.1 M or 1.0 M HCl. Solutions of 2.6 μmol NAD^+ free acid in 2.9 mL of 0.05 M NaCl were acidified with 0.1 mL of 0.1 M HCl prior to titration against 0.1 M NaOH. We obtained pK_a values of 3.35 ± 0.05 for NAD^+ and of 3.65 ± 0.05 for NADH at an ionic strength of 0.05 mol kg^{-1}.

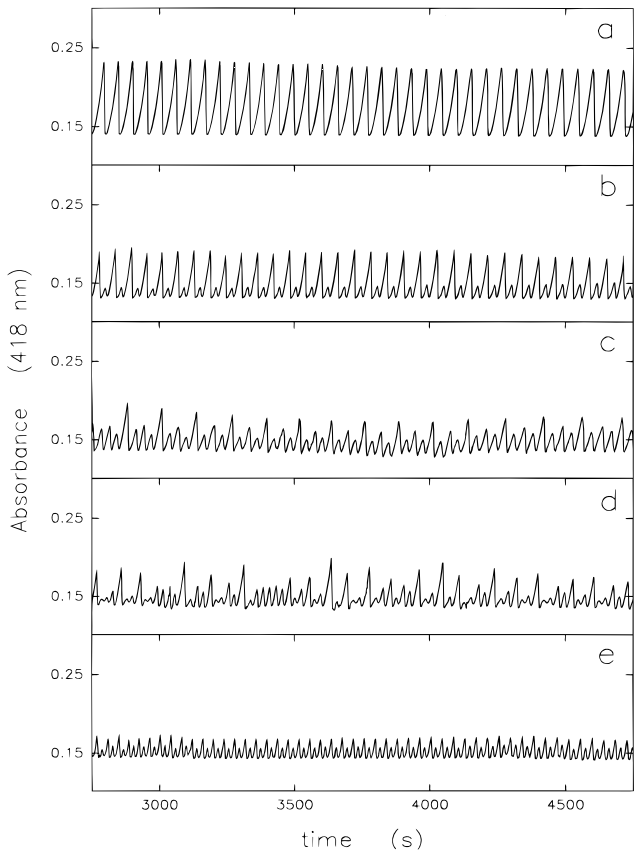

Figure 1. Period-doubling route to chaos at pH 5.2. The response to increasing NADH concentration level is as follows: (a) p_1 state, (b) p_2 state, (c), p_4 oscillations, (d) chaos, and ***(e)*** p_2* oscillations. The mean NADH concentrations corresponding to the different states are (a) 65 μM, (b) 73 μM, (c) 75 μM, (d) 76 μM, and (e) 81 μM.

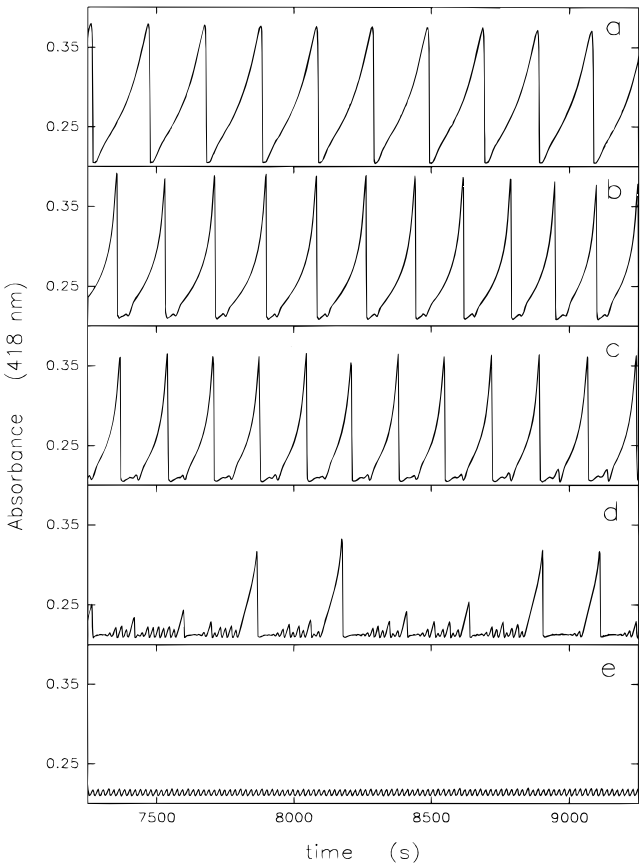

Figure 2. Period-adding sequence at pH 6.3. The response to increasing NADH concentration level is as follows: (a) 1^0 oscillations, (b) 1^1 mixed-mode oscillations, (c), 1^2 state, (d) chaos, and (e) 0^1 oscillations. The NADH mean concentrations corresponding to the different states are (a) 105 μM, (b) 113 μM, (c) 118 μM, (d) 125 μM, and (e) 128 μM.

Horseradish peroxidase (RZ 3.0), NADH disodium salt, and NAD^+ free acid were purchased from Boehringer Mannheim; methylene blue from Merck, and 2,4-dichlorophenol from Aldrich.

III. Experimental Results

1. Low pH Experiments. At pH 5.2, the response to increasing NADH levels is a series of *period-doubled* states,[37] followed by a region of chaotic dynamics, which gives way to small amplitude oscillations by way of reverse bifurcations (Figure 1). In detail, we first observe period-1 oscillations (labeled p_1; Figure 1a), which are then transformed into period-2 (p_2; Figure 1b) and later into period-4 cycles (p_4; Figure 1c). Upon a further increase in the NADH level, chaotic behavior is observed (Figure 1d). The bifurcation sequence is thus compatible with period-doubling to chaos, *i.e.*, period-1 → period-2 → period-4 → ... → chaos, where the states represented by the symbols "→ ... →" may or may not actually exist. A similar route to chaos was previously reported by Geest *et al.*[13] at pH 5.1 using the concentration of DCP as the control parameter.

With further increases in NADH concentration, the system exits the chaotic region through a series of reverse period-doublings. First, one observes small-amplitude period-2 oscillations (p_2*, Figure 1e), which are then replaced by period-1 oscillations (p_1*, not shown) of even smaller amplitude and, finally, a stationary state (not shown). Overall, the amplitude of the oscillations decreases with increasing concentrations of NADH.

2. High pH Experiments. At pH 6.3, the response to increases in the mean NADH concentration conforms to a *period-adding* sequence.[10] Representative time series are displayed in Figure 2. At low concentrations of NADH, only simple periodic oscillations are observed (Figure 2a). Following the L^S notation, where L and S indicate the number of large- and small-amplitude excursions per repeating unit, we label these oscillations 1^0. At higher concentrations of NADH, the 1^0 cycles give way to 1^1 mixed-mode oscillations (MMO's, Figure 2b), which, in turn, are replaced by 1^2 MMO's (Figure 2c) and then, with still further increases in NADH concentration, by 1^3 and 1^4 states (not shown). With increasing S, there is a reduction in the range of parameter values corresponding to the individual MMO's.

Beyond the region of period-adding, *i.e.*, with additional increases in the level of NADH, the system enters a chaotic regime (Figure 2d). With further increases in the mean NADH concentration, chaos gives way to small-amplitude period-2 cycles (not shown), which we label 0^2. Reverse bifurcations occasioned by again increasing the concentration of NADH result in 0^1 cycles (Figure 2e) and, finally, a stationary state. Closer inspection of the transitions between pairs of neighboring MMO's, 1^S and 1^{S+1}, reveals that the 1^S state loses stability via period-doubling. Thus, very narrow windows of period-doubled and chaotic behavior are found at these transitions. The complete sequence of dynamical states at pH 6.3 is displayed schematically in Figure 3 and discussed in detail by Hauser and Olsen.[10]

Comparing the bifurcation sequences obtained at pH 5.2 and 6.3, we note the following:

1. In both cases, there is a decrease in cycle amplitude with increasing levels of NADH concentration.

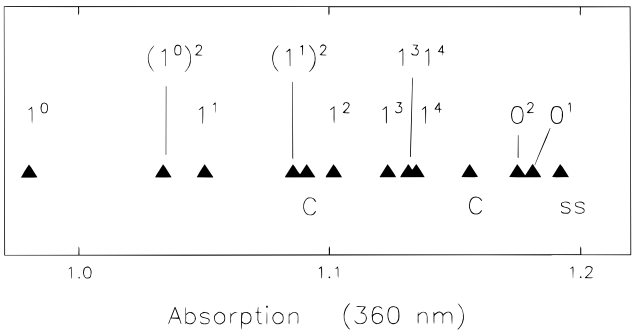

Figure 3. Experimentally observed state diagram at pH 6.3. The absorbance at 360 nm monitors the mean NADH concentration. Periodic MMO states are labeled according to the L^S notation. C indicates chaos. The exact location of the individual states, as well as the value of their maximal amplitudes, is subject to experimental uncertainty.

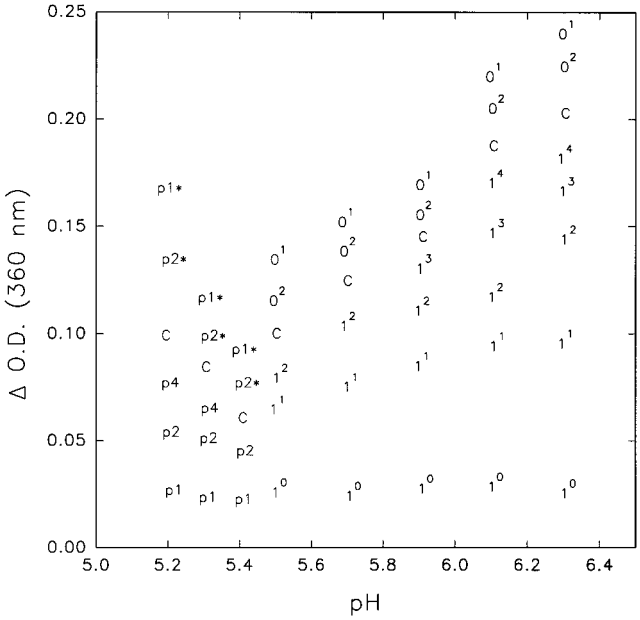

Figure 4. Sequence of periodic states leading to chaos for different pH values. The dynamic states observed at pH 5.4 are labeled p_1, p_2, C, p_2*, and p_1*. Alternatively, these states can be labeled 1^0, 1^1, C, 0^2, and 0^1, respectively (see text). In order to clarify the narrowing of the region of complex dynamics at pH 5.4, the sequences of states are plotted as a function of the absorbance at 360 nm (monitors the NADH concentration) relative to a skew (but linear) baseline which has origin at $A_{360} = 0.62$ at pH 5.2 and $A_{360} = 0.96$ at pH 6.3.

2. The chaotic region following the 1^S MMO's is exited by a reverse period-doubling cascade involving small-amplitude oscillations.

3. The transition to a stationary state at high NADH concentrations seems to occur via a supercritical Hopf bifurcation.

3. From Period-Adding to Period-Doubling. To study the transition from period-doubling to period-adding, the preceding experiments were repeated at intermediate pH values. The results are summarized in Figure 4, where, for clarity, we indicate only the cycles of base period, *i.e.*, we omit period-doubled and chaotic states between adjacent MMO's.

At pH 6.1, all of the states observed at pH 6.3 are still observable, but the NADH concentrations corresponding to the individual MMO's have narrowed. The parameter range corresponding to chaotic oscillations is also somewhat smaller. As the pH is further decreased from 6.1 to 5.5 in steps of 0.2 pH units, the range of NADH concentrations corresponding to the different MMO's continues to shrink with the concomitant disappearance of the higher period MMO's. Thus at pH 5.9, the most complex MMO is the 1^3 cycle, whereas at pH 5.7, the cycle of greatest period is the 1^2 oscillation. These changes are accompanied by continuing compression of the chaotic region and, although it is not readily discernable from the figure, by a decrease in cycle amplitude.

At pH 5.4, the main chaotic domain has shrunk to a very narrow interval. In addition, the most complex periodic state is a 2-cycle. Moreover, the amplitude of the large component of the period-2 cycle has dwindled to the point that it can be described either as a 1^1 MMO cycle or as a cycle of period-2, *i.e.*, distinguishing between period-adding or period-doubling states is no longer possible at this pH.

As the reaction medium is further acidified, one observes the reappearance of more complex oscillations. At pH 5.3, the chaotic region is somewhat broader and is preceded by period-4 transients (in addition to stable cycles of period-1 and period-2). At pH 5.2, the period-4 cycles becomes stable and the chaotic region continues to broaden. One is tempted to conjecture that cycles of even higher period might be observed with additional reductions in pH. Unfortunately, such conjectures must remain a matter of speculation, since, at pH <5.0, the decomposition of NADH becomes substantial.[41,42] This acidic decomposition is not very well understood and hence effectively alters the entire reaction system in a not well-defined direction.

In sum, the transition from period-adding to period-doubling occurs at a pH of approximately 5.4 and involves the following phenomena: (i) narrowing of the ranges of NADH concentrations corresponding to the various dynamic states, (ii) loss of the periodic states of greatest complexity preceding the transition to chaos; and (iii) continuous decrease in the amplitude of oscillations corresponding to a given dynamic state. Factors (i) and (ii) give the experimentally-determined control diagram a decidedly wasp-waisted appearance (Figure 4). On either side of the transition point, the diagram expands as additional periodic states become resolvable and the ranges of NADH concentrations corresponding to the different dynamical regimes broaden.

IV. Computer Simulations

Complementing experimental studies of the PO reaction is a growing number of mechanistic models[1,7,15,38,43−54] which seek to provide a mathematical accounting of its behavior. All of these schemes are rooted in the work of Yokota and Yamazaki,[43] who, along with Fed'kina *et al.*[44−46] and Degn and Olsen,[5,55−57] were the first to attempt to capture the reaction mathematically. Here, we assess the ability of the recently proposed BFSO scheme[58] (Table 1) to reproduce the experimental results described in section III. We stress that the numerics were undertaken not only to test the model but also to inform our interpretation of the experimental findings. The latter are *per force* incomplete by comparison with what can be generated by a mathematical model, and they leave unresolved certain details regarding some of the dynamical states and the transitions between them. Among these is the nature of the transitional regions between adjacent MMO's at high pH and whether or not "period-doubling to chaos" for pH <5.4 corresponds to the Feigenbaum scenario discussed in section I.

The dynamics of chemical reactions may be studied by altering the concentrations of the reactants or by varying pH or temperature. In the case of the PO reaction, potential control parameters include the concentrations of peroxidase,[12] MB,[14] DCP,[13,30] and NADH (this study and ref 10), the oxygen equilibrium concentration,[8,9] and pH (this study and ref 37).

TABLE 1: Elementary Steps in the PO Reaction[a]

reaction	R_i	constant
1. $NADH + O_2 + H^+ \xrightarrow{k_1} NAD^+ + H_2O_2$	$k_1[NADH][O_2]$	$k_1 = 3\ M^{-1}\ s^{-1}$
2. $H_2O_2 + Per^{3+} \xrightarrow{k_2} coI$	$k_2[H_2O_2][Per^{3+}]$	$k_2 = 1.8 \times 10^7\ M^{-1}\ s^{-1}$
3. $coI + NADH \xrightarrow{k_3} coII + NAD^\bullet$	$k_3[coI][NADH]$	$k_3 = 4.0 \times 10^4\ M^{-1}\ s^{-1}$
4. $coII + NADH \xrightarrow{k_4} Per^{3+} + NAD^\bullet$	$k_4[coII][NADH]$	$k_4 = 2.6 \times 10^4\ M^{-1}\ s^{-1}$
5. $NAD^\bullet + O_2 \xrightarrow{k_5} NAD^+ + O_2^-$	$k_5[NAD^\bullet][O_2]$	$k_5 = 2.0 \times 10^7\ M^{-1}\ s^{-1}$
6. $O_2^- + Per^{3+} \xrightarrow{k_6} coIII$	$k_6[O_2^-][Per^{3+}]$	$k_6 = 1.7 \times 10^7\ M^{-1}\ s^{-1}$
7. $2O_2^- + 2H^+ \xrightarrow{k_7} H_2O_2 + O_2$	$k_7[O_2^-]^2$	$k_7 = 2.0 \times 10^7\ M^{-1}\ s^{-1}$
8. $coIII + NAD^\bullet \xrightarrow{k_8} coI + NAD^+$	$k_8[coIII][NAD^\bullet]$	$k_8 = 9.0 \times 10^7\ M^{-1}\ s^{-1}$
9. $2NAD^\bullet \xrightarrow{k_9} (NAD)_2$	$k_9[NAD^\bullet]^2$	k_9 = variable
10. $Per^{3+} + NAD^\bullet \xrightarrow{k_{10}} Per^{2+} + NAD^+$	$k_{10}[Per^{3+}][NAD^\bullet]$	$k_{10} = 1.8 \times 10^6\ M^{-1}\ s^{-1}$
11. $Per^{2+} + O_2 \xrightarrow{k_{11}} coIII$	$k_{11}[Per^{2+}][O_2]$	$k_{11} = 1.0 \times 10^5\ M^{-1}\ s^{-1}$
12. $NADH(stock) \xrightarrow{k_{12}} NADH(liquid)$	$k_{12}[NADH]_{st}$ = variable	
13. $O_2(gas) \underset{k_{-13}}{\overset{k_{13}}{\rightleftharpoons}} O_2(liquid)$	$k_{13}[O_2]_{eq} = 7.2 \times 10^{-8}\ M\ s^{-1}$	
	$k_{-13}[O_2]$	$k_{-13} = 6.0 \times 10^{-3}\ s^{-1}$

[a] The different oxidation steps of the enzyme are ferric peroxidase (Per^{3+}), ferrous peroxidase (Per^{2+}), compound I (coI), compound II (coII), and compound III (coIII). For the differential equations see ref 10.

Although easy to implement experimentally, the use of pH and temperature as control parameters makes for difficulties when one attempts to interpret the results. This is because changing these parameters has multiple effects on the reaction mechanism, with virtually every rate constant being affected to one degree or another. With regard to changing pH under assumptions corresponding to the experimental conditions, exploratory calculations (not reported here) suggest that k_9 appears to have the most significant effects on the reaction's dynamics. We propose that the basis of this observation is as follows:

At pH values between 2 and 7, both NADH and $NAD^\bullet$ carry net negative charges. NADH, $NAD^\bullet$, and NAD^+ are subject to pH-dependent protonation/deprotonation, as reflected by their pK_a values (pK_a = 3.65 and 3.35 for NADH and NAD^+, respectively). Changes in pH will affect the rate constants of elementary steps in which these nucleotides participate. A particularly strong effect is expected for reactions involving two of these nucleotides. In BFSO (Table 1), this is the case for reaction R9. We thus expect that a decrease in pH will lead to a reduction in net negative charge on $NAD^\bullet$ and hence an increase in k_9 due to reduced Coulombic repulsion between $NAD^\bullet$ molecules (see the discussion) similar to the disproportionation of superoxide.[59]

Accordingly, we simulate reductions in pH from 6.3 to 5.2 by increasing k_9 from 4.0×10^7 to $8.0 \times 10^7\ M^{-1}\ s^{-1}$. For a series of k_9 values in this range, bifurcation diagrams were computed by varying the inflow rate of NADH from 1.0×10^{-7} to $1.33 \times 10^{-7}\ M\ s^{-1}$, with the remaining constants set to the values indicated in Table 1. Initial conditions are given in Table 2. For computational details, see Bronnikova *et al.*[38]

TABLE 2: Initial Conditions for Simulations (in μM)

$[NADH]_0 = 0.0$	$[O_2]_0 = 12.0$	$[NAD^\bullet]_0 = 0.0$
$[Per^{3+}]_0 = 1.5$	$[coI]_0 = 0.0$	$[coII]_0 = 0.0$
$[coIII]_0 = 0.0$	$[H_2O_2]_0 = 0.0$	$[O_2^-]_0 = 0.0$
$[Per^{2+}]_0 = 0.0$		

1. Bifurcation Diagrams. Figure 5a shows the "high pH" simulation ($k_9 = 4.0 \times 10^7\ M^{-1}\ s^{-1}$). Here, we see periodic windows corresponding to elements 2−5 of a period-adding sequence (1^1−1^4 MMO's. Not visible is the 1^0 state, which occurs at much lower input rates of NADH, *e.g.*, at $k_{12}[NADH]_0 = 5.9 \times 10^{-8}\ M\ s^{-1}$). Between the windows, one observes narrow regions of complex dynamics. Interestingly, these regions are preceded by equally narrow regions of period-doubling. Beyond the 1^4 window (Figure 5a), a region of apparently chaotic dynamics precedes a narrow reverse cascade, which, in turn, gives way to a stable fixed point (not shown).

Figure 5d shows the corresponding situation for the "low-pH" simulation ($k_9 = 8.0 \times 10^7\ M^{-1}\ s^{-1}$). Here, one observes period-1, -2, and -4 cycles, followed by a region of chaotic dynamics which, in turn, gives way to a reverse cascade.

Bifurcation diagrams corresponding to "intermediate" pH values of $k_9 = 4.8 \times 10^7\ M^{-1}\ s^{-1}$ and $k_9 = 7.0 \times 10^7\ M^{-1}\ s^{-1}$ are shown in Figure 5b,c. Representative time series (compare with Figures 1 and 2) for the high- and low-pH simulations are displayed in Figures 6 and 7.

2. Comparison with Experiments. Taken together, the simulations evidence substantial agreement with the experi-

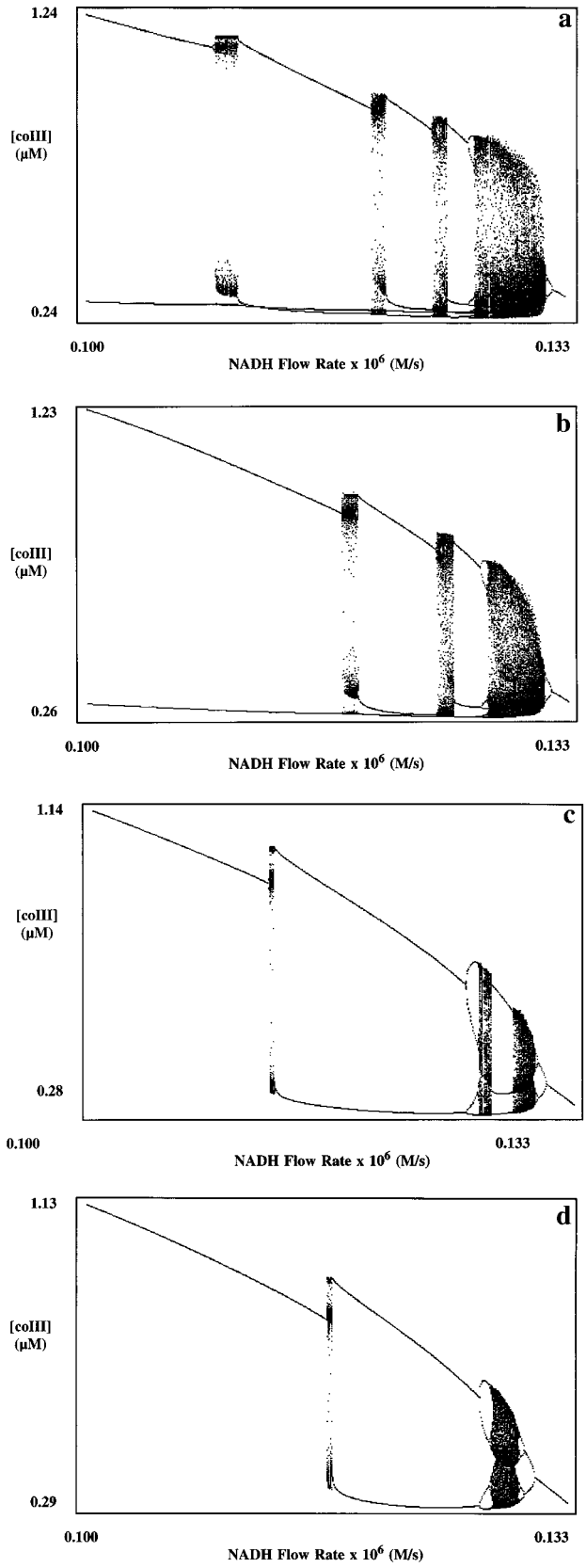

Figure 5. Simulated bifurcation scenarios induced by BFSO. The control parameter is the rate of NADH input. Diagrams arranged in order of decreasing simulated pH. (a) $k_9 = 4.0 \times 10^7$ M^{-1} s^{-1}. (b) $k_9 = 4.8 \times 10^7$ M^{-1} s^{-1}. (c) $k_9 = 7.0 \times 10^7$ M^{-1} s^{-1}. (d) $k_9 = 8.0 \times 10^7$ M^{-1} s^{-1}.

mental results. The major qualitative discrepancy is the model's inability to reproduce the experimentally observed narrowing of the control diagram at intermediate pH values. On the other hand, the predicted ordering of the dynamical states is consistent

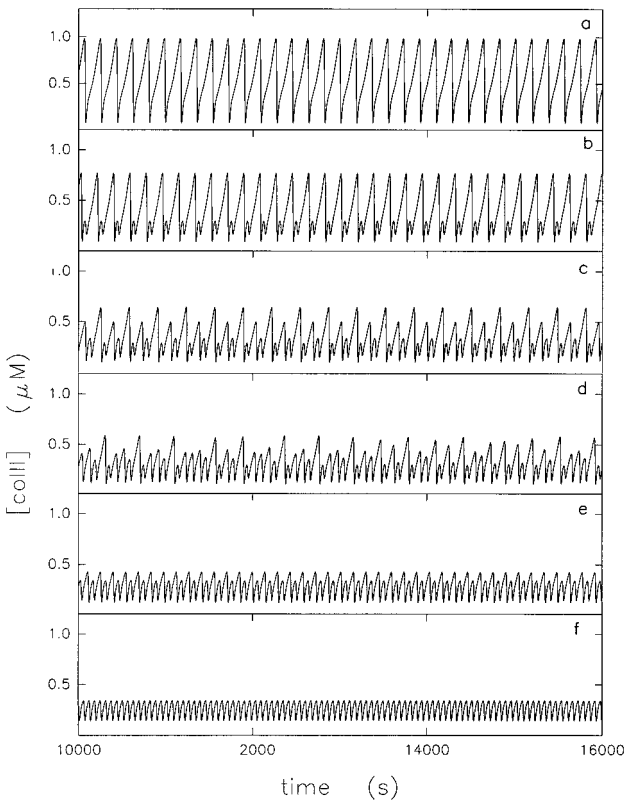

Figure 6. Simulated time series of compound III concentrations for $k_9 = 8 \times 10^7$ M^{-1} s^{-1} ("low pH"). The response to increases in the NADH inflow rate, k_{12}, is as follows: (a) p_1 state at $k_{12}[NADH]_{st} = 1.08 \times 10^{-7}$ M s^{-1}; (b) p_2 state at $k_{12}[NADH]_{st} = 1.22 \times 10^{-7}$ M s^{-1}; (c) p_4 state at $k_{12}[NADH]_{st} = 1.27 \times 10^{-7}$ M s^{-1}; (d) chaos at $k_{12}[NADH]_{st} = 1.29 \times 10^{-7}$ M s^{-1}; (e) p_2* state at $k_{12}[NADH]_{st} = 1.30 \times 10^{-7}$ M s^{-1}; (f) p_1* state at $k_{12}[NADH]_{st} = 1.32 \times 10^{-7}$ M s^{-1}. Compare with Figure 1.

with the data. Especially gratifying is the loss of the higher order MMO's with increasing k_9 (decreasing pH) and the observation of narrow regions of period-doubling between the windows. Moreover, in all cases, the simulations evidence decreasing cycle amplitude with increased NADH input (Figures 6 and 7), which pattern is clearly discernable in Figures 1 and 2. As to quantitative comparisons, the predicted reactant concentrations (and the corresponding flow rates) for the most part differ from their experimental counterparts by less than 50%, in which regard, the principal disparity is the fact that the 1^0 cycle for the high-pH simulation is obtained at rates of NADH input far lower than the minimum in Figure 5a.

Of course, bifurcation diagrams of the sort shown in Figure 5 must be interpreted with care. In the present instance, examination of the corresponding time series reveals significant anomalies *vis-à-viz* the experimental data. The basis for this assertion is shown in Figures 6 and 7. In Figure 6, we display the period-1 through period-4 cycles, a chaotic time series, and the small amplitude period-2 and period-1 oscillations (*i.e.*, p_2* and p_1*, respectively) for the "low-pH" simulation. In Figure 7, we display four mixed mode oscillations, 1^0, 1^1, 1^2, and 1^3, followed by a chaotic time series and, finally, the small amplitude 0^1 cycle for the "high-pH" sequence. Comparison with Figures 1 and 2 reveals the following discrepancies:

1. The absolute frequencies of oscillation are discordant. Specifically, the predicted periods exceed those of the experimental cycles, typically, by a factor of 3.

2. For the experimental time series, one can convincingly make the point that at low pH the oscillations preceding the transition to chaos are of type p_n (see above), whereas at high

pH the corresponding cycles observed are of type 1^S, *i.e.*, mixed-mode. For the simulations, this distinction is not nearly so clear-cut.

3. Especially for the simulated "mixed-mode" oscillations (Figure 7), the wave-form is wrong. More precisely, following a major excursion, the experimental time series drop directly to a minimum from which they gradually increase. In the simulations, there is no such loitering. Put another way, in the experimental system, trajectories appear to be injected more closely to the vicinity of a fixed point, from which neighborhood they escape more slowly (see Hauser and Olsen[10] for discussion).

V. Discussion

In the present paper, we have presented the results of a detailed experimental study of peroxidase−oxidase dynamics at different pH values. We have also attempted to account for the experimental results in terms of a detailed model,[38] by changing a *single* rate constant. The choice of the rate constant for the dimerization of the NAD$^\bullet$ radical (k_9) as a proxy parameter for pH, is based on two considerations:

(i) NAD$^\bullet$ carries two negative charges at neutral pH. After protonation, the number of negative charges decreases to one. Thus, similar to the dismutation of superoxide (R7), reaction R9 in Table 1 is really three reactions involving NAD$^\bullet$ radicals with different net charges:

$$\mathrm{NAD}^{\bullet(1-)} + \mathrm{NAD}^{\bullet(1-)} \rightarrow (\mathrm{NAD})_2^{(2-)} \qquad \text{(R9a)}$$

$$\mathrm{NAD}^{\bullet(1-)} + \mathrm{NAD}^{\bullet(2-)} \rightarrow (\mathrm{NAD})_2^{(3-)} \qquad \text{(R9b)}$$

$$\mathrm{NAD}^{\bullet(2-)} + \mathrm{NAD}^{\bullet(2-)} \rightarrow (\mathrm{NAD})_2^{(4-)} \qquad \text{(R9c)}$$

Of these, (R9c) will dominate at high pH, since at this pH most of the NAD$^\bullet$ will be deprotonated to NAD$^{\bullet(2-)}$. Reaction R9c is also the reaction with the smallest rate constant due to a higher Coulombic repulsion compared to reactions R9a and R9b. The pK values of NAD$^\bullet$ are presumably similar to those reported here for NADH and NAD^+ (3.65 and 3.35 respectively). Under this assumption, the fraction of NAD$^{\bullet(1-)}$ is approximately 10% at pH 5.2 and less than 1% at pH 6.3. Direct measurements of the pH-dependence of k_9 have not yet been reported, but an estimate based on the assumptions made above suggest that the value of k_9 increases at least twofold when the pH is decreased from 6.3 to 5.2. (We remark parenthetically that the value of $k_9 = 5.6 \times 10^7\ \mathrm{M^{-1}\ s^{-1}}$ reported in the literature[60,61] was measured at pH 6.4 which is close to the value for which we observe period-adding.)

(ii) Although virtually all of the model's rate constants probably depend on pH, numerical explorations suggest that the dynamics of BFSO are most sensitive to changes in k_9. This is despite the fact that reactions R1 and R7 are obviously pH-dependent (Table 1). For example, even though the disproportionation rate of superoxide radicals (R7) is known[59] to vary considerably with pH over the range of values considered here, simulations indicate that the dynamics are but moderately sensitive to changes in k_7.

As a first approximation, it therefore seems reasonable to simulate the effect of pH by changing only k_9.

As previously noted, the principal objectives of the present study were (i) to characterize the transition from period-doubling to period-adding in what has become a model system for studying complex biochemical dynamics and (ii) to determine the extent to which the experimental findings can be reproduced by a detailed model. With regard to the first objective, we

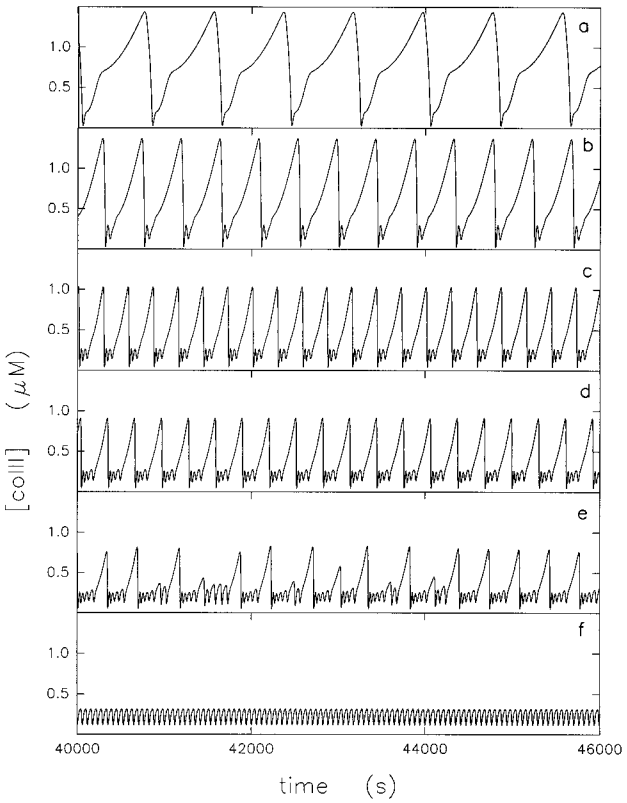

Figure 7. Simulated time series of compound III concentrations for $k_9 = 4 \times 10^7\ \mathrm{M^{-1}\ s^{-1}}$ ("high pH"). The response to increases in the NADH inflow rate, k_{12}, is as follows: (a) 1^0 state at $k_{12}[\mathrm{NADH}]_{st} = 5.95 \times 10^{-8}\ \mathrm{M\ s^{-1}}$; (b) 1^1 state at $k_{12}[\mathrm{NADH}]_{st} = 8.5 \times 10^{-8}\ \mathrm{M\ s^{-1}}$; (c) 1^2 MMO's at $k_{12}[\mathrm{NADH}]_{st} = 1.15 \times 10^{-7}\ \mathrm{M\ s^{-1}}$; (d) 1^3 MMO's at $k_{12}[\mathrm{NADH}]_{st} = 1.22 \times 10^{-7}\ \mathrm{M\ s^{-1}}$; (e) chaos at $k_{12}[\mathrm{NADH}]_{st} = 1.28 \times 10^{-7}\ \mathrm{M\ s^{-1}}$; (f) 0^1 state at $k_{12}[\mathrm{NADH}]_{st} = 1.33 \times 10^{-7}\ \mathrm{M\ s^{-1}}$. Compare with Figure 2.

observed that the transition from one bifurcation scenario to the other is marked by characteristic changes in the sequence of dynamical states which is obtained on varying a representative control parameter. What remains to be determined is the context in which these changes—loss of dynamical complexity, narrowing of the chaotic region, *etc.*—can be expected to occur. In this regard, it has been reported[62] that reducing k_9 also induces a shift from period-doubling to period-adding in response to increasing k_8. It has been argued that increasing k_8 in BFSO is interpretable as increasing the concentration of DCP,[38,62] essentially because DCP is known to stimulate the conversion of compound III to compound I.[63,64] Thus, further tests of the validity of the BFSO scheme could be to repeat the experiments of Geest *et al.*,[38] using the concentration of DCP as a bifurcation parameter, to test if pH induces a similar transition from period-doubling to period-adding. More generally, we note that both period-doubling and MMO scenarios have been reported for a three-variable extension of the abstract autocatalator.[65,66]

With regard to our second objective, it is apparent that the BFSO model as implemented here can reproduce many, but not all, of the major experimental findings. The lack of complete agreement between model and experiment may reflect one or more of the following: 1. The model omits one or more important features of the real PO mechanism. 2. Some of the parameter values (Table 1) are wrong. 3. The decision to model changing pH by adjusting the value of a *single* rate constant is too simplistic.

Regarding the first point, potentially trouble-making features of the model include the omission of the oxidation of NADH by superoxide radicals, a step which was included in the original

scheme of Yokota and Yamazaki,[43] and the absence of explicit reactions involving MB and DCP. In BFSO, the latter compounds enter only via their effect on the rate constants, k_1 and k_8. As for the rate constants themselves, it is well known that several of the values in Table 1, like many other rate constants in the chemical literature, are little better than order of magnitude guesses. Finally, and as noted above, variations in pH can be expected to have multiple effects on the reaction mechanism, an expectation which may not be well mimicked by our decision to examine only the consequences of varying a *single* rate constant. In short, there are many potential sources of error, with the consequence that considerable work remains.

To conclude, we note that the simulations raise questions as to the correct interpretation of the transition from period-1 to period-2 dynamics at low pH. In this regard, the experimental picture is one of conventional period-doubling, *i.e.*, the transition appears to be a smooth one, whereas the model predicts an abrupt change in cycle amplitude with an intervening region of complex behavior (see Figure 5d). Thus, there are two possibilities: On the one hand, the discrepancy may simply be another instance in which the BFSO model as implemented here fails to give exact agreement with experiment, *i.e.*, for higher values of k_9, one observes smooth doublings of the period-1 cycle. Alternatively, a region of complex dynamics may, in fact, exist between p_1 and p_2 but be so narrow as to resist experimental resolution. We emphasize that the discrepancy, if it is real, pertains only to low pH values (5.2−5.3). At higher values (5.5≤ pH ≤6.3), the predicted transitional regions are observed experimentally. Similar regions have also been reported for the Belousov−Zhabotinsky reaction, in which case their significance has been the subject of considerable dispute[67,68]—see, for example the discussion by Petrov *et al.*[66] In the second article in this series,[39] we consider these regions in greater detail, focusing on the mathematical events that give rise to the complex dynamics observed therein. In brief, we suggest that the associated dynamics are, in fact, chaotic and that they result from homoclinic transitions to chaos involving the destruction of period-doubled tori.

Acknowledgment. M.H. and L.F.O. acknowledge financial support by the Danish Natural Science Research Council, the Carlsberg Foundation, and the Novo Nordisk Foundation. We thank Thomas Graf, Søren Knudsen, and Lars Teil Nielsen for assistance with the construction of the experimental setup and data acquisition and Anita Lunding for help with the experiments, as well as Alexander Scheeline, Raima Larter, and Sheryl Hemkin for sending preprints of their manuscripts. T.V.B. and W.M.S. thank Michael Cusanovich for encouragement and support.

References and Notes

(1) Larter, R.; Olsen, L. F.; Steinmetz, C. G.; Geest, T. In *Chaos in Chemistry and Biochemistry*; Field, R. J., Györgyi, L., Ed.; World Scientific: Singapore, 1993; pp 175−224.

(2) Degn, H. *Nature* **1968**, *217*, 1047−1050.

(3) Aguda, B. D.; Frisch, L.-L. H.; Olsen, L. F. *J. Am. Chem. Soc.* **1990**, *112*, 6652−6656.

(4) Nakamura, S.; Yokota, K.; Yamazaki, I. *Nature* **1969**, *222*, 794.

(5) Olsen, L. F.; Degn, H. *Biochim. Biophys. Acta* **1978**, *523*, 321−334.

(6) Fed'kina, V. R.; Bronnikova, T. V.; Ataullakhanov, F. I. *Studia Biophys.* **1981**, *82*, 159 −164.

(7) Fed'kina, V. R.; Ataullakhanov, F. I.; Bronnikova, T. V. *Theor. Exptl. Chem.* **1988**, *24*, 165−172.

(8) Hauck, T.; Schneider, F. W. *J. Phys. Chem*. **1993**, *97*, 391−397.

(9) Hauck, T.; Schneider, F. W. *J. Phys. Chem.* **1994**, *98*, 2072−2077.

(10) Hauser, M. J. B.; Olsen, L. F. *J. Chem. Soc. Faraday Trans.* **1996**, *92*, 2857−2863.

(11) Samples, M. S.; Hung, Y.-F.; Ross, J. *J. Phys. Chem.* **1992**, *96*, 7338−7343.

(12) Olsen, L. F.; Degn, H. *Nature* **1977**, *267*, 177−178.

(13) Geest, T.; Steinmetz, C. G.; Larter, R.; Olsen, L. F. *J. Phys. Chem*. **1992**, *96*, 5678−5680.

(14) Hauser, M. J. B.; Olsen, L. F. In *Plant Peroxidases: Biochemistry and Physiology*; Obinger, C., Burner, U., Ebermann, R., Penel, C., Grepin, H., Eds.; University of Geneva: Geneva, 1996; pp 82−87.

(15) Olson, D. L.; Williksen, E. P.; Scheeline, A. *J. Am. Chem. Soc.* **1995**, *117*, 2−15.

(16) Kummer, U.; Valeur, K. R.; Baier, G.; Wegmann, K.; Olsen, L. F. *Biochim. Biophys. Acta*, **1996**, *1289*, 397−403.

(17) Kummer, U.; Hauser, M. J. B.; Wegmann, K.; Olsen, L. F.; Baier, G. *J. Am. Chem. Soc.* **1997**, *119*, 2084−2087.

(18) Guckenheimer, J.; Holmes, P. *Nonlinear Oscillations, Dynamical Systems and Bifurcations of Vector Fields*; Springer-Verlag: New York, 1983.

(19) Jackson, E. A. *Perspectives of Nonlinear Behavior*; Cambridge University Press: Cambridge, UK, 1989, 1990; Vol. 1, 2.

(20) Wiggens, S. *Introduction to Applied Nonlinear Dynamical Systems and Chaos*; Springer-Verlag: New York, 1990.

(21) Marek, M.; Schreiber, I. *Chaotic Behaviour of Deterministic Dissipative Systems*; Academia: Prague, 1991.

(22) May, R. M. *Nature* **1976**, *261*, 459−467.

(23) Feigenbaum, M. J. *J. Stat. Phys.* **1978**, *19*, 25−52.

(24) Feigenbaum, M. J. *J. Stat. Phys.* **1979**, *22*, 186−223.

(25) Collet, P.; Eckmann, J.-P. *Iterated Maps on the Interval*; Birkhäuser: Boston, 1980.

(26) Jakobsen, M. V. *Commun. Math. Phys.* **1981**, *81*, 39−88.

(27) The well-known result[26] is this: parameter values corresponding to chaotic itineraries have positive Lebesque measure but do not form subintervals.

(28) Metropolis, N.; Stein, M.; Stein, P. *J. Combinat. Theory* **1973**, *15*, *25−44*.

(29) Metropolis, Stein, and Stein consider the mapping, T_λ: $X \rightarrow \lambda F(X)$, subject to the following hypotheses: (i) $F(X)$ is piecewise continuous and strictly positive on (0,1); (ii) $F(0) = F(1) = 0$; (iii) $F()$ has a unique maximum at $X^* \in (0,1)$. The applicability of their result is therefore more limited than is often supposed.

(30) Steinmetz, C. G.; Geest, T.; Larter, R. *J. Phys. Chem.* **1993**, *97*, 5649−5653.

(31) Bergé, P.; Pomeau, Y.; Vidal, C., *Order Within Chaos: Towards a Deterministic Approach to Turbulence*; J. Wiley & Sons: NY, 1986.

(32) Thompson, J. M. T.; Stewart, H. B. *Nonlinear Dynamics and Chaos*; J. Wiley & Sons: NY, 1986.

(33) Arnol'd, V. I. *Funct. Anal. Appl.* **1977**, *11*, 1−10.

(34) Aronson, D. G.; Chory, M. A., Hall, A. McGehee, R. P. *Commun. Math. Phys.* **1981**, *83*, 303−351.

(35) For cycles, ρ is rational, and the ratio, p/q, may be interpreted as the number of revolutions, p, about the loop required to visit all q points of the cycle.

(36) Ringland, J.; Issa, N.; Schell, M. *Phys. Rev. A* **1990**, *41*, 4223−4235.

(37) Hauser, M. J. B.; Andersen, S.; Olsen, L. F. In: *Plant Peroxidases: Biochemistry and Physiology*; Obinger, C., Burner, U., Ebermann, R., Penel, C., Grepin, H., Eds.; University of Geneva: Geneva, 1996; pp 88−93.

(38) Bronnikova, T. V.; Fed'kina, V. R.; Schaffer, W. M.; Olsen, L. F. *J. Phys. Chem*. **1995**, *99*, 9309−9312.

(39) Bronnikova, T. V.; Schaffer, W. M.; Hauser, M. J. B.; Olsen, L. F. Routes to Chaos in the Peroxidase-Oxidase Reaction: the Fat Torus Route. Manuscript in preparation.

(40) Olson, D. L.; Scheeline, A. *J. Phys. Chem.* **1995**, *99*, 1204−1211.

(41) Miksic, J. R.; Brown, P. R. *Biochemistry* **1978**, *17*, 2234−2238.

(42) Olson, D. L.; Scheeline, A. *Anal.Chim. Acta* **1993**, *283*, 703−717.

(43) Yokota, K.; Yamazaki, I. *Biochemistry* **1977**, *16*, 1913−1920.

(44) Fed'kina, V. R.; Ataullakhanov, F. I.; Bronnikova, T. V.; Balabaev, N. K. *Studia Biophys.* **1978**, *72*, 195−202.

(45) Fed'kina, V. R.; Bronnikova, T. V.; Ataullakhanov, F. I. In *Posters: 1st All-Union Biophysical Congress, Acad. Sci. USSR, Moscow*, **1982**, *2*, 152.

(46) Fed'kina, V. R.; Ataullakhanov, F. I.; Bronnikova, T. V. *Biophys. Chem.* **1984**, *19*, 259−264.

(47) Fed'kina, V. R.; Bronnikova, T. V. In Summaries of Reports to All-Union Conference on Self-Organization in Physical, Chemical and Biological Systems. *Synergetics-86*; Shtiintsa: Kishinev; 1986; p 126.

(48) Aguda, B. D.; Larter, R. *J. Am. Chem. Soc.* **1990**, *112*, 2167−2174.

(49) Aguda, B. D.; Larter, R. *J. Phys. Chem.* **1991**, *95*, 7913−7916.

(50) Fed'kina, V. R.; Bronnikova, T. V.; Ataullakhanov, F. I. *Biofizika* **1992**, *37*, 885−894.

(51) Fed'kina, V. R.; Bronnikova, T. V. *Biofizika* **1995**, *40*, 36−47.

(52) Hung, Y.-F.; Schreiber, I.; Ross, J. *J. Phys. Chem.* **1995**, *99*, 1980−1987.

(53) Larter, R.; Hemkin, S. *J. Phys. Chem.* **1996**, *100*, 18924−18930.

(54) Schreiber, I.; Hung, Y.-F.; Ross, J. *J. Phys. Chem.* **1996**, *100*, 8556−8566.
(55) Degn, H.; Olsen, L. F.; Perram, J. W. *Ann. NY Acad. Sci.* **1979**, *316*, 623−637.
(56) Olsen, L. F. *Z. Naturforsch.* **1979** *34a*, 1544−1546.
(57) Olsen, L. F. *Phys. Lett. A* **1983**, *94*, 454−457.
(58) Historically, the BFSO scheme derives from the Urbanalator[14] from which it differs by the *inclusion* of reactions 10 and 11. Both BFSO and the Urbanalator differ from most earlier detailed models by *omission* of the oxidation of NADH by superoxide, O_2^-, and by *inclusion* of the oxidation of NADH by molecular oxygen (R1).
(59) Bielski, B. H. J.; Allen, A. O. *J. Phys. Chem.* **1977**, *81*, 1048−1050.
(60) Scheeline, A.; Olson, D. L.; Williksen, E. P.; Horras, G. A.; Klein, M. L.; Larter, R. *Chem. Rev.* **1997**, *97*, 739−756.
(61) Land, E. J.; Swallow, J. *Biochim. Biophys. Acta* **1971**, *234*, 34−42.
(62) Bronnikova, T. V.; Schaffer, W. M.; Olsen, L. F. *J. Chem. Phys.* **1996**, *105*, 10849−10859.
(63) Watanabe, N.; Inaba, H. *Photochem. Photobiol.* **1993**, *57*, 570−576.
(64) Halliwell, B. *Planta* **1978**, *140*, 81−88.
(65) Peng, B.; Scott, S. K.; Showalter, K. *J. Chem. Phys.* **1990**, *94*, 5243−5246.
(66) Petrov, V.; Scott, S. K.; Showalter, K. *J. Chem. Phys.* **1992**, *97*, 6191−6198.
(67) Schneider, F. W.; Münster, A. F. *J. Phys. Chem*. **1991**, *95*, 2130−2138.
(68) Györgyi, L.; Field, R. J.; Noszticzius, Z.; McCormick, W. D.; Swinney, H. L. *J. Phys. Chem.* **1992**, *96*, 1228−1233.